ANALYSIS OF LUMPED AND DISTRIBUTED ELEMENTS MODELS OF CUT MUSCLE FIBERS IN VASELINE OR SUCROSE GAP PREPARATIONS

FRANCESCO ANDRIETTI, GIOVANNI BERNARDINI, AND ANTONIO PERES
Dipartimento di Fisiologia e Biochimica Generali and Dipartimento di Biologia, Universitá di Milano, 20133 Milano, Italy

ABSTRACT A general method of finding the time course and the steady state distribution of potential in Vaseline or sucrose gap preparations is given by making use of the linear cable equation. The general solution has been found analytically in terms of its Laplace transform and then numerically inverted. Two particular experimental situations, namely the single gap and the double gap preparations, have been analyzed. The results have been compared with the solutions of the commonly used lumped elements models. While for the double gap no large errors are introduced by the lumped model, for the single gap there are significant differences. The dependence of the voltage distribution on various electrical and geometrical parameters has been examined. It is suggested that the proposed mathematical treatment might be used by experimenters as a reference to assess the validity of simplified lumped models.

INTRODUCTION

The technique of voltage clamping a cut skeletal muscle fiber placed in Vaseline or sucrose gaps offers important advantages such as the possibility of introducing different substances in the fiber interior (Kovacs and Schneider, 1978; Kovacs et al., 1979), or of allowing the fiber to contract (Horowicz and Schneider, 1981; Jaimovich et al., 1982). Both techniques are based on the idea of separating through electrical insulations different parts of the fiber. Under ideal conditions, this allows one to inject a current and to measure the membrane potential difference without making use of microelectrodes. The two methods differ in the way the insulations are realized, either with a thin strip of Vaseline or with a slender stream of sucrose solution, but in both cases, a cable having segments with different electrical characteristics is obtained.

In spite of the wide use of these techniques, a general analytical treatment of the electrical behavior of these models does not exist, except in some particular cases or at steady state (Jirounek and Straub, 1971; Jirounek et al., 1981; McGuigan and Tsien, 1974). Lumped elements models are frequently used, but these models have the obvious limitation of considering circuit elements of finite (instead of infinitesimal) length. The aim of our work is to offer a method to solve such problems in a more general way in order to test under which experimental conditions and to what extent the simplified lumped elements models are applicable without significant errors.

The effect of the presence of the T-tubules has been studied in the preceding paper (Andrietti and Bernardini, 1984) and it has been shown that the longitudinal spread of electrotonic potential in a muscular fiber is well approximated by an equivalent model whose electrical parameters are the apparent resistances and capacities, as may be, for example, determined from voltage clamp experiments.

THE DISTRIBUTED MODEL

In terms of the theory developed in the preceding paper (Andrietti and Bernardini, 1984), the part of a skeletal muscle fiber placed in an experimental chamber for Vaseline or sucrose gap voltage clamp can be represented by the modular circuit of Fig. 1. In each kth section the space and time dependence of the voltage is described by the well-known partial differential equation (see e.g., Jack et al., 1975)

$$\lambda_k^2 \frac{\partial^2 V_k}{\partial x_k^2} = \tau_k \frac{\partial V_k}{\partial t} + V_k, \tag{1}$$

where λ_k and τ_k are the apparent time and space constants, $V_k = V_{k,i} - V_{k,e}$ is the difference between the internal and external potentials in the kth section, l_k is the length of the kth section, and $0 \leq x_k \leq l_k$.

Eq. 1 represents a system of partial differential equations connected through their boundary conditions. For the continuity of the potential, one has

$$V_k(l_k^-, t) = V_{k+1}(0^+, t). \tag{2}$$

A second group of boundary conditions concerns the values of the derivative of the potential at the end points of the sections. Let us indicate with I_i and I_e the internal and external currents, and with $r_{k,i}$ and $r_{k,e}$ the internal and

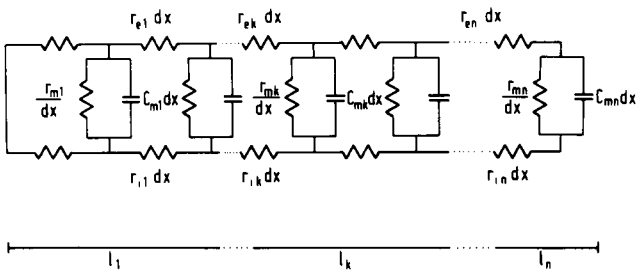

FIGURE 1 Modular circuit representing the portion of a skeletal muscle fiber in an experimental chamber with insulating gaps. Each section k (1–n) represents the part of the fiber either in a gap or in a conducting pool.

external resistances; one obtains

$$\frac{\partial V_{k,i}}{\partial x_k} = -r_{k,i}I_i; \frac{\partial V_{k,e}}{\partial x_k} = -r_{k,e}I_e,$$

so that

$$\frac{\partial V_k}{\partial x_k} = -r_{k,i}I_i + r_{k,e}I_e;$$

$$\frac{\partial V_{k+1}}{\partial x_{k+1}} = -r_{k+1,i}I_i + r_{k+1,e}I_e.$$

From the last two relations, letting $I = I_i + I_e$, one obtains, after some calculations, the second group of boundary conditions:

$$\left(\frac{\partial V_{k+1}}{\partial x_{k+1}}\right)_{0^+} = \left(\frac{\partial V_k}{\partial x_k}\right)_{l_k^-} \frac{r_{k+1,i} + r_{k+1,e}}{r_{k,i} + r_{k,e}} + \frac{r_{k+1,e}I^+(r_{k,i} + r_{k,e}) - r_{k,e}I^-(r_{k+1,i} + r_{k+1,e})}{r_{k,e} + r_{k,i}} \quad (3)$$

where I^- and I^+ indicate the limit values of I at the left and right side of the kth section end.

When in $x_1 = 0$ the cable is short circuited, the corresponding initial condition will be $V_1(0, t) = 0$. The last boundary condition will depend on the terminal situations of the cable and will change according to the experimental arrangement.

To determine the solution of Eq. 1, let us indicate with $\bar{V}_k(x, s)$ the Laplace transform of $V_k(x, t)$ with respect to time. Taking into account the initial condition $V_1(x, 0) = 0$, one has

$$\lambda_k^2 \frac{\partial^2 \bar{V}_k}{\partial x_k^2} = \tau_k s \bar{V}_k + \bar{V}_k,$$

whose general solution is

$$\bar{V}_k(x, s) = A_k(s) \exp[-x_k\phi_k(s)/\lambda_k] + B_k(s) \exp[x_k\phi_k(s)/\lambda_k], \quad (4)$$

where $\phi(s) = (\tau_k s + 1)^{1/2}$.

If we let

$$X_{2k-1}(s) = A_k(s), \qquad X_{2k}(s) = B_k(s),$$

the functions $X_i(s)$ ($i = 1, 2, ..., 2n$) have to be determined by taking into account the linear system of order $2n$ obtained from Eq. 4 and from the boundary conditions given above, rewritten in terms of their Laplace transforms. We obtain

$$\begin{bmatrix} a_{1,1}(s) \cdots a_{1,2n}(s) \\ \cdots\cdots\cdots\cdots \\ \cdots\cdots\cdots\cdots \\ \cdots\cdots\cdots\cdots \\ a_{2n,1}(s) \cdots a_{2n,2n}(s) \end{bmatrix} \cdot \begin{bmatrix} X_1(s) \\ \cdots \\ \cdots \\ \cdots \\ X_{2n}(s) \end{bmatrix} = \begin{bmatrix} c_1(s) \\ \cdots \\ \cdots \\ \cdots \\ c_{2n}(s) \end{bmatrix} \quad (5)$$

The values of the coefficients $a_{i,j}(s)$, $c_i(s)$, are given by the boundary conditions considered above. For the first $n - 1$ rows of the matrix ($1 \leq i < n$), we will obtain from Eqs. 2 and 4

$$a_{i,j}(s) = 0 \qquad \text{for } j < 2i - 1,\ j > 2i + 2;$$

$$a_{i,2i-1}(s) = \exp[-l_i\phi_i(s)/\lambda_i];$$

$$a_{i,2i}(s) = \exp[l_i\phi_i(s)/\lambda_i];$$

$$a_{i,2i+1}(s) = a_{i,2i+2}(s) = -1;$$

$$c_i(s) = 0.$$

From row n to row $2n - 2$ ($n \leq i < 2n - 1$), the coefficients $a_{i,j}(s)$ will be determined from Eqs. 3 and 4:

$$a_{i,j}(s) = 0 \quad \text{for } j < 2(i - n) + 1, j > 2(1 - n) + 4;$$

$$a_{i,2(i-n)+1}(s) = -\frac{\phi_{i-n+1}(s)}{\lambda_{i-n+1}} \frac{r_{i-n+2,i} + r_{i-n+2,e}}{r_{i-n+1,i} + r_{i-n+1,e}} \cdot \exp[-l_{i-n+1}\phi_{i-n+1}(s)/\lambda_{i-n+1}];$$

$$a_{i,2(i-n)+2}(s) = \frac{\phi_{i-n+1}(s)}{\lambda_{i-n+1}} \frac{r_{i-n+2,i} + r_{i-n+2,e}}{r_{i-n+1,i} + r_{i-n+1,e}} \cdot \exp[l_{i-n+1}\phi_{i-n+1}(s)/\lambda_{i-n+1}];$$

$$a_{i,2(i-n)+3}(s) = \phi_{i-n+2}(s)/\lambda_{i-n+2};$$

$$a_{i,2(i-n)+4}(s) = -\phi_{i-n+2}(s)/\lambda_{i-n+2};$$

$$c_i(s) = -\frac{r_{i-n+2,e}I^+(r_{i-n+1,i} + r_{i-n+1,e}) - r_{i-n+1,e}I^-(r_{i-n+2,i} + r_{i-n+2,e})}{r_{i-n+1,e} + r_{i-n+1,i}}.$$

The coefficients of the last two rows are determined according to the end conditions of the cable. Because of the short circuit in $x_1 = 0$, one has

$$a_{2n-1,1}(s) = a_{2n-1,2}(s) = 1;$$

$$a_{2n-1,j}(s) = 0 \qquad \text{for } j > 2;$$

$$c_{2n-1}(s) = 0.$$

The values of $a_{2n,j}(s)$ and $c_{2n}(s)$ will change according to the particular experimental arrangement.

At steady state, Eq. 1 becomes

$$\lambda_k^2 \frac{d^2V_k}{dx_k^2} = V_k,$$

whose general solution is

$$V_k(x) = A_k \exp(-x_k/\lambda_k) + B_k \exp(x_k/\lambda_k). \quad (6)$$

The coefficients A_k and B_k are determined according to the linear system obtained from Eq. 6 and from the boundary conditions given above as has been seen for $A_k(s)$ and $B_k(s)$.

We will consider in detail two particular cases: single and double Vaseline gap. To give some numerical results, we will adopt the following rounded values of electrical parameters taken from Hodgkin and Nakajima (1972), corresponding to a fiber of 80 μm in diameter: $r_i = 3.4$ MΩ/cm, $r_m = 120$ k$\Omega \cdot$ cm, $c_m = 0.15$ μF/cm.

The experimental arrangement used by Kovacs and Schneider (1978) may be represented by the electrical model of Fig. 2 *A*. In this case, $n = 2$, $r_{m,1} = r_{m,2} = r_m$; $r_{1,e} = r_e$; $r_{2,e} = 0$, $r_{1,i} = r_{2,i} = r_i$; $\tau_{m,1} = \tau_{m,2} = \tau_m$. The value of the external resistance, r_e, the length of the gap, l_1, and of the muscle fiber out of the gap l_2, taken from Kovacs and Schneider (1978), are rounded to 280 MΩ/cm, 600 μm, and 400 μm, respectively. In this case, Eq. 5 becomes a system of four linear equations whose coefficients can be determined according to what we have said above. Because the effect of the termination of the cable, one has

$$\left(\frac{\partial V_2}{\partial x_2}\right)_{l_2^-} = 0.$$

This boundary condition enables us to determine the coefficients

$$a_{4,1}(s) = a_{4,2}(s) = 0;$$
$$a_{4,3}(s) = -[\phi_2(s)/\lambda_2] \exp[-l_2\phi_2(s)/\lambda_2];$$
$$a_{4,4}(s) = [\phi_2(s)/\lambda_2] \{\exp[l_2\phi_2(s)/\lambda_2]\};$$
$$c_4(s) = 0.$$

Solving Eq. 5, we have obtained the values of $A_1(s)$, $B_1(s)$, $A_2(s)$, $B_2(s)$, which have been introduced in Eq. 4 to find the Laplace transform of the potential. In Fig. 3 *A* ,the results of the numerical inversion obtained with the method given in the preceding paper (Andrietti and Bernardini, 1984) are presented. Because of the linear properties of the model, with respect to the stimulating current I, the value of the potential in Fig. 3 *A* and in the following figures has been given in arbitrary units. The corresponding steady state values obtained from Eq. 6 are shown in Fig. 4 *A*, *C*, *D*.

The experimental arrangement for double Vaseline gap can be represented by the electrical model of Fig. 2 *B*. In this case: $n = 3$, $r_{1,e} = r_{3,e} = r_e$, $r_{2,e} = 0$, $r_{m,1} = r_{m,2} = r_{m,3} = r_m$; $r_{1,i}$, $= r_{2,i} = r_{3,i} = r_i$, $\tau_{m,1} = \tau_{m,2} = \tau_{m,3} = \tau_m$. The dimensions of the walls separating the pools (l_1 and l_3) and of the central pool (l_2), taken from Kovacs et al. (1979) are, respectively, 250 and 700 μm, the other parameters being unchanged. As the central pool is grounded, $I = 0$ for $x > l_1$. In this case, Eq. 5 becomes a system of six linear equations whose coefficients are determined as explained previously. Because of the short-circuit effect at the end of the cable, one has $a_{6,5}(s) = \exp[-l_3\phi_3(s)/\lambda_3]$, $a_{6,6}(s) = \exp[l_3\phi_3(s)/\lambda_3]$, $a_{6,j}(s) = 0$, for $j < 5$, $c_6(s) = 0$. Solving Eq. 5, we have obtained the values of $A_1(s)$, $B_1(s)$, $A_2(s)$, $B_2(s)$, $A_3(s)$, $B_3(s)$, which have been introduced in Eq. 4 to find the Laplace transform of the potential that has been inverted as in the case of the single gap. The numerical

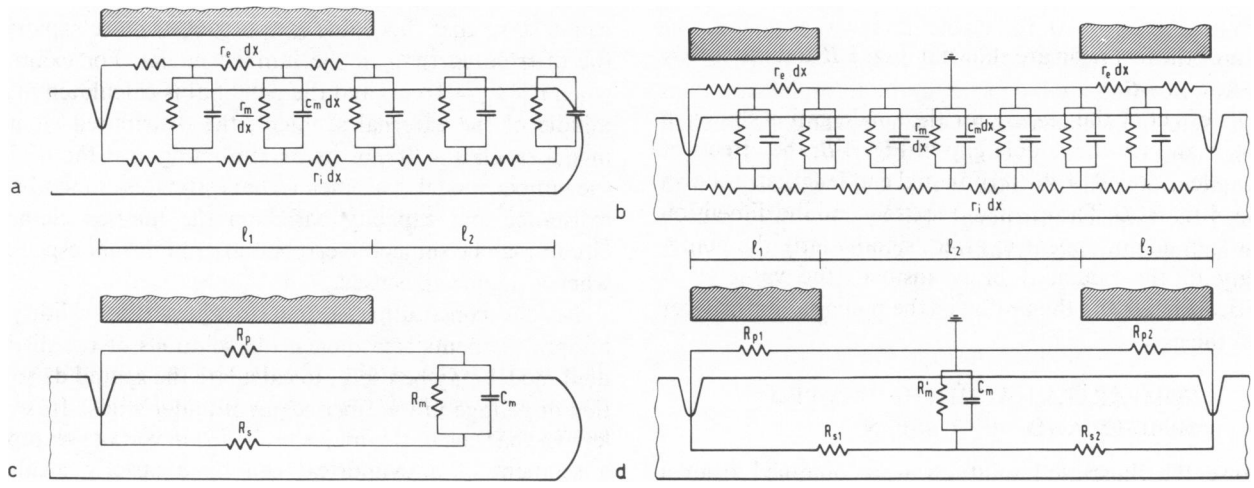

FIGURE 2 Distributed model of a single (*a*) and double (*b*) Vaseline gap and lumped elements circuit for a single (*c*) and double (*d*) Vaseline gap. Dashed areas represent the insulation gaps. Indentations in the fiber are short circuits between inside and outside. In all cases, the site of current injection is at the extreme left of the circuit ($x_1 = 0$). The membrane properties under study are always those of unit l_2.

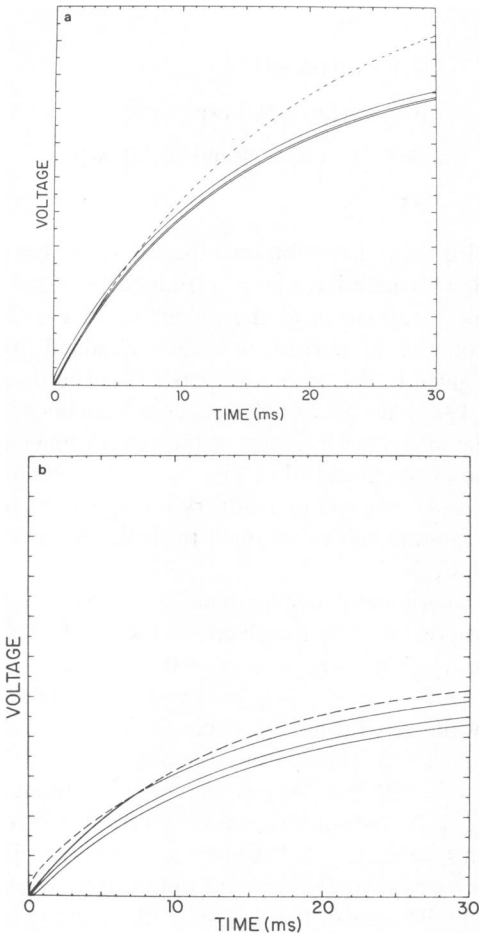

FIGURE 3 The three continuous curves have been obtained by numerically inverting Eq. 4 for the single (*a*) and double (*b*) Vaseline gap, and represent the time course of voltage at the beginning, at the middle, and at the end of the fiber segment outside the gap (l_2 in Fig. 2) because of the same rectangular step of stimulating current. The dashed lines represent the corresponding lumped elements model solutions given by Eqs. 7 and 8. The values of the parameters are given in the text.

results of the inversion are shown in Fig. 3 *B* and the steady state in Fig. 4 *B*.

The effect of the sealing for the single gap is shown in Fig. 4 *A* and for the double gap in Fig. 4 *B*; the effects of the gap length and of the terminated end length are shown in Fig. 4 *C* and *D*. The quality of the seal and the dimension of the gap do not appear to affect significantly the homogeneity of the potential in l_2; instead, the value of l_2 significantly affects the profile of the potential in the fiber out of the gap.

COMPARISON WITH THE LUMPED MODELS AND DISCUSSION

Because the illustrated solutions were obtained from a nonsimplified model, they are assumed to be a more faithful representation of the real situation than other solutions obtained from simplified models. It is clear that the method outlined here is not very practical for the interpretation of the experimental results, but it might be useful as a reference to estimate the extent of the errors introduced by different kinds of simplifications. As the values of the geometrical and electrical parameters may vary strongly, depending on the experimental arrangement, and may vary among different experiments performed with the same technique, a general comparison between distributed and lumped elements models is not possible here, but, as an example, we have examined the behaviors of the lumped models of Fig. 2 *C* and *D*, and we have compared them with the results given by our method. In response to a step current pulse, I_s, the time courses of membrane potential for single (V') and for double (V'') gap are

$$V'(t) = \frac{R'_m R_p}{R'_m + R_p + R_s}\,[1 - \exp(-t/\tau')] \cdot I_s; \qquad (7)$$

$$V''(t) = \frac{R_{p1}\,[1 - \exp(-t/\tau'')]\,I_s}{(R_{s1} + R_{p1})\left[\dfrac{1}{R_{s1} + R_{p1}} + \dfrac{1}{R'_m} + \dfrac{1}{R_{s2} + R_{p2}}\right]}, \qquad (8)$$

where $\tau' = R'_m C'_m$ and

$$\tau'' = \frac{C'_m}{\dfrac{1}{R_{s1} + R_{p1}} + \dfrac{1}{R'_m} + \dfrac{1}{R_{s2} + R_{p2}}}.$$

For comparison between the distributed (Fig. 2) and lumped (Fig. 3) models: $R'_m = r_m/l_2$; $R_p = r_e\, l_1$; $R_s = r_i\,(l_1 + l_2/2)$; $R_{p1} = r_e l_1$; $R_{p2} = r_e l_3$; $R_{s1} = r_i\,(l_1 + l_2/2)$; $R_{s2} = r_i\,(l_3 + l_2/2)$; $C'_m = c_m \cdot l_2$.

In Fig. 3 *A* and *B*, the dashed lines represent Eqs. 7 and 8. In Fig. 4 *A* and *B*, the asymptotic values of Eqs. 7 and 8 are reported. While for the double gap case there are no large differences, the situation is worse for the single gap system. Besides the difference in the steady state level, one can observe that this value is approached more rapidly in the distributed than in the lumped model. For example, when $t = \tau_m = 18$ ms and the potential is calculated in the middle of the external segment, the distributed element model reaches ~70% of its maximum against the 63% of the lumped model. This means that estimates of membrane resistance and capacity based on the lumped elements circuit may be subject to errors that are relevant especially when a single gap is used.

Besides constituting a tool to check the validity of lumped elements treatments, the solutions of the distributed model may be useful to calculate the spatial distribution of voltage in the fiber segment under study. It is well known that one of the major problems in voltage-clamping a segment of a cylindrical cell by a strictly localized current source is the spatial uniformity of the potential. While it has been already shown, and it is also easy to understand, that the length of the segment to be clamped is

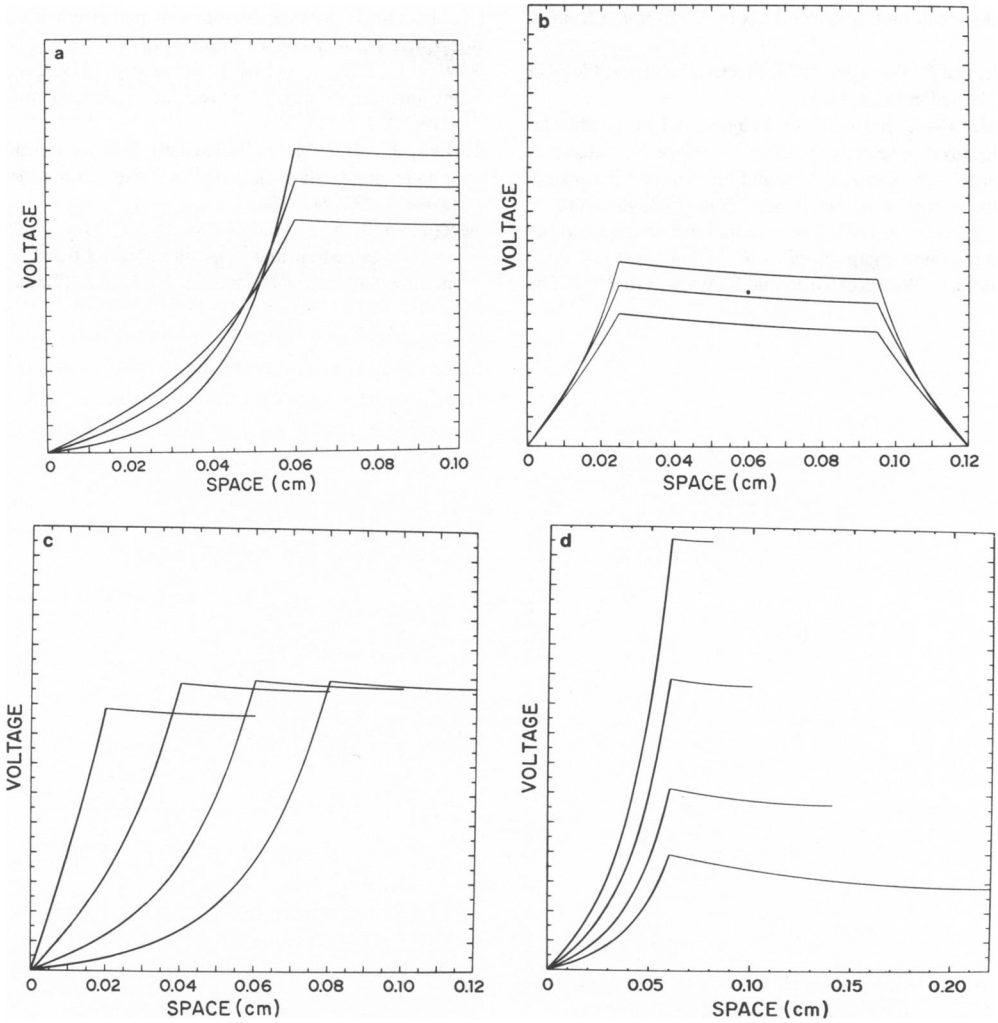

FIGURE 4 Steady state solutions of the distributed model for the single (*a*, *c*, *d*) and double (*b*) Vaseline gap for the same rectangular pulse of stimulating current. (*a* and *b*) Effect of changing the value of the gap resistance: lower curves, r_e = 140 MΩ/cm; intermediate curves, r_e = 280 MΩ/cm; upper curves, r_e = 560 MΩ/cm. The other parameters are the same as Fig. 3; the dots represent the steady state values of the lumped elements circuit whose transient behavior is shown in Fig. 3 *a* and *b*, and must be compared with the level of the intermediate curves in the middle of the exposed segment. (*c*) Effect of changing l_1; other parameters are equal to the ones of Fig. 3 *a*. (*d*) Effect of changing l_2; other parameters are equal to the ones of Fig. 3 *a*.

of primary importance, it is more difficult to evaluate the effects of other geometrical and electrical parameters. Fig. 4 shows the solutions of the distributed model when the length of the fiber, the length of the insulating gap, and the resistance of the gap are changed. Except for the already mentioned effect of the fiber length (Fig. 4 *D*), it is apparent that both gap length (Fig. 4 *C*) and gap resistance (Fig. 4 *A* and *B*) do not have a great influence on the spatial distribution at steady state. This last result is of particular importance because, while the length of the various segments may be rather easily adjusted by the experimenter, the quality of the insulating seals is difficult to be standardized.

We have analyzed in detail two particular experimental situations, but the proposed method, with slight modifications to take into account different boundary conditions, could be applied to more complex systems as, for example, the three Vaseline gap preparation used by Hille and Campbell (1976).

Received for publication 17 May 1983 and in final form 26 January 1984.

REFERENCES

Andrietti, F., and G. Bernardini. 1984. Segmented and "equivalent" representation of the cable equation. *Biophys. J.* 46:615–623.

Hille, B., and T. Campbell. 1976. An improved Vaseline gap voltage-clamp for skeletal muscle fibers. *J. Gen. Physiol.* 67:265–293.

Hodgkin, A. L., and S. Nakajima. 1972. The effect of diameter on the electrical constants of frog skeletal muscle fibers. *J. Physiol. (Lond.).* 221:105–120.

Horowicz, P., and M. F. Schneider. 1981. Membrane charge movement

in contracting and noncontracting skeletal fibers. *J. Physiol.* (*Lond.*). 314:565–593.

Jack, J. B., D. Noble, and R. W. Tsien. 1975. Electrical Current Flows in Excitable Cells. Clarendon Press, Oxford.

Jaimovich, E., M. Ildefonse, J. Barhanin, O. Rougier, and M. Lazdunski. 1982. Centruroides toxin, a selective blocker of surface Na^+ channels in skeletal muscle: voltage-clamp analysis and biochemical characterization of the receptor. *Proc. Natl. Acad. Sci. USA.* 79:3896–3900.

Jirounek, P., and R. W. Straub. 1971. The potential distribution and the short-circuiting in the sucrose gap. *Biophys. J.* 11:1–10.

Jirounek, P., G. J. Jones, C. W. Burckhardt, and R. W. Straub. 1981. The correction factors for sucrose gap measurements and their practical application. *Biophys. J.* 33:107–119.

Kovacs, L., E. Rios, and M. F. Schneider. 1979. Calcium transients and intramembrane charge movement in skeletal muscle fibers. *Nature* (*Lond.*). 279:391–396.

Kovacs, L., and M. F. Schneider. 1978. Contractile activation by voltage-clamp depolarization of cut skeletal muscle fibers. *J. Physiol.* (*Lond.*). 277: 483–506.

McGuigan, J. A. S., and R. W. Tsien. 1974. Some limitations of the double sucrose gap, and its use in a study of the slow outward current in mammalian ventricular muscle. *J. Physiol.* (*Lond.*). 240:775–806.